AIAA JOURNAL
Vol. 42, No. 10, October 2004

Nanoplate Model for Platelike Nanomaterials

Haitao Zhang* and C. T. Sun†
Purdue University, West Lafayette, Indiana 47907

A plate model is developed for nanostructured materials possessing platelike geometry, such as ultrathin films. The dispersion relations of a three-layered nanomaterial are analyzed with both the nanoplate model and the lattice model to show the effectiveness of this nanoplate model. Cylindrical bending of a three-atom-layered nanoplate is analyzed with the nanoplate model, the lattice model, and the continuum Mindlin plate theory. It is found that the nanoplate model predicts the deflection in good agreement with the lattice model. The continuum Mindlin plate theory tends to underpredict the deflection. This result indicates that, if the continuum plate theory is used to extract the Young's modulus of a nanomaterial, the value could be significantly underestimated.

I. Introduction

NANOTECHNOLOGY is considered the most promising and challenging technology to be explored. Recently, many efforts have been made to develop and apply materials at the scale of nanometers. Some promising applications have already begun to emerge. Among them, ultrathin polymethylmethacrylate films have been used to store information up to 500 Gbit/in.[2], which is about 40–50 times more than today's best research demonstrations with magnetic recording.[1] Nanotube has been used as nanoprobes in scanning tunneling microscope,[2] atomic force microscope,[3] and transistor components.[4] Those applications have also brought new challenging problems in analyzing mechanical properties of materials at the scale of nanometers.

Although conventional continuum mechanics, including structure mechanics such as beam, plate, and shell theories, has been the dominant tool for modeling materials and structures, the validity of its applications in modeling mechanical behavior of emerging nanomaterials and structures/devices composed of nanomaterials[5,6] has been questioned. For example, continuum mechanics have been often employed in the data analysis of experiments involving nanomaterials with questionable results.[7] Molecular mechanics is a natural tool for simulating materials at the nanoscale. However, its capability is limited by its need of extraordinary computing power. To aid the future development of nanotechnology, it is essential that new tools be developed that offer the simplicity of continuum mechanics and the ability to account for the nanoscale characteristics of the material.[8]

Platelike nanomaterials are materials that have nanometer dimensions in the thickness direction. Ultrathin films, nanolaminates, and platelets in nanoclay are good examples. For this type of nanomaterials, their large in-plane dimensions justify the use of the continuum description in the plane to achieve simplicity. The discrete atomic characteristics in the thickness direction must be retained. Along this path, a semicontinuum model has been recently proposed by Zhang and Sun[9] for platelike nanomaterials. In this model, the discrete property along the thickness is retained while the in-plane dimensions are treated with the classical continuum approach. With this model, Sun and Zhang[10] have investigated the size dependence of Young's modulus and Poisson's ratios of platelike nanomaterials and found that elastic moduli of materials are size dependent at the nanoscale. Their prediction of size-dependent Young's modulus was consistent with some experimental observations.[11]

In the present paper, the aforementioned semicontinuum model is used to develop a nanoplate theory that can predict the response of platelike nanomaterials under external loading. The equations of motion are first derived with Hamilton's principle. Dispersion relations of harmonic wave propagation in a three-layered nanomaterial are then analyzed with the nanoplate model and the lattice model to evaluate the accuracy of the nanoplate model. Finally, possible pitfalls in using the classical continuum theory to interpret experimental data on nanomaterials are discussed.

II. Field Equations

Consider a rectangular platelike nanostructured material of uniform thickness as shown in Fig. 1. The x and y axes are in the midplane. The discrete points represent atoms. The distance between two atoms is referred to as a. Along the thickness, there are $2N + 1$ atom layers. Henceforth, layer number indicates the total number of atom layers in the thickness direction of the nanomaterial. The in-plane dimensions of the material are assumed to be very large compared to the atomic spacing. Each atom interacts with its nearest and next-nearest neighbors, and the interactions are represented by force constants α_1 and α_2 (Fig. 2), respectively.[12] Although an ideal cubic structure is chosen for this study, the approach proposed in this paper can be readily extended to nanomaterials with other crystal structures.

In this paper, we ignore the difference between spring constants for surface atoms and interior atoms. Moreover, we do not consider three-body and many-body interactions. Ignoring such interactions may result in the Cauchy symmetry in effective continuum moduli. This deficiency may be reduced by incorporating a third force constant to account for the effect of three-body forces.[13] However, the effective Young's moduli and Poisson's ratios for face-centered cubic (FCC) materials obtained based on the lattice model with these simplifying assumptions seem to agree with those obtained with the molecular mechanics simulation with the embedded-atom-method potentials.[14]

The resulting components of translational displacement at an arbitrary atom located at (x, y, and la, where l is an integer) are denoted by $u_l\ (x, y, t)$, $v_i\ (x, y, t)$, and $w_i\ (x, y, t)$, whereas the corresponding components at the midplane are $u(x, y, t)$, $v\ (x, y, t)$, and $w(x, y, t)$. Similar to the development of Mindlin's plate theory[15] the displacements of atoms in the lth layer are approximated with the following two-term expansions:

$$u_i(x, y, t) = u(x, y, t) - la\psi_x(x, y, t) \tag{1a}$$

$$v_i(x, y, t) = v(x, y, t) - la\psi_y(x, y, t) \tag{1b}$$

$$w_i(x, y, t) = w(x, y, t) - lav(u_{,x} + v_{,y}) \tag{1c}$$

Presented as Paper 2002-1316 at the AIAA/ASME/ASCE/AHS/ASC 43rd Structures, Structural Dynamics, and Materials Conference, Denver, CO, 22–25 April 2002; received 17 September 2003; revision received 10 May 2004; accepted for publication 10 May 2004.

*Graduate Student, School of Aeronautics and Astronautics, 315 North Grant Street. Member AIAA.

†Neil A. Armstrong Distinguished Professor, School of Aeronautics and Astronautics, 315 North Grant Street. Fellow AIAA.

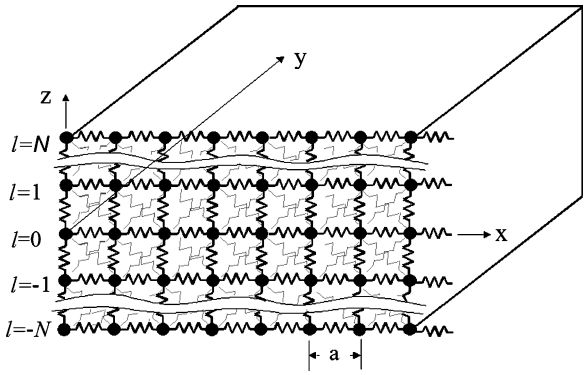

Fig. 1 Platelike nanomaterial.

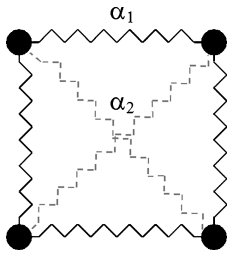

Fig. 2 Nearest and next-nearest neighbor interactions of a selected element in the *x*–*z* section.

in which ψ_x and ψ_y can be interpreted as the rotations of the cross sections of the nanoplate and $v = \alpha_2/(\alpha_1 + \alpha_2)$ is Poisson's ratio for cubic nanomaterials with three layers of atoms.[10] The second term in on the right-hand side of Eq. (1c) represents the displacement in the thickness direction that results from in-plane deformations ε_x and ε_y through Poisson's effect.

A. Strain Energy, Kinetic Energy, and Work of External Loads

In this section, the total kinetic energy T, strain energy U, and work of external loading , W, of the nanomaterial are derived. The kinetic energy and strain energy are obtained in the same manner as described in Refs. 9 and 10. First, the kinetic energy in the nanoplate can be obtained from the approximate nanoplate displacements given by Eq. (1). We have

$$T = \frac{\rho a}{2}\sum_{l=-N}^{N}\int\int_A \left[(\dot{u} - la\dot{\psi}_x)^2 + (\dot{v} - la\dot{\psi}_y)^2 + (\dot{w} - lav\dot{u}_{,x} - lav\dot{v}_{,y})^2\right] dx\,dy \tag{2}$$

where a dot denotes differentiation with respect to time, A is in-plane area of the nanoplate, and ρ is the mass density defined as

$$\rho = m/a^3 \tag{3}$$

in which m is the mass of a lattice point (an atom).

The total strain energy U is obtained as

$$\begin{aligned}
U = {} & \int\int_A \left[N\alpha_2(1-v)^2 + (\alpha_1+\alpha_2)\left(Nv^2 + N + \frac{1}{2}\right)\right]u_{,x}^2\,dx\,dy \\
& + \int\int_A \left[N\alpha_2(1-v)^2 + (\alpha_1+\alpha_2)\left(Nv^2 + N + \frac{1}{2}\right)\right]v_{,y}^2\,dx\,dy \\
& + \int\int_A \left[\sum_{i=0}^{N-1}\alpha_1(l+1)^2a^2 + \sum_{i=0}^{N-1}\frac{3}{2}\alpha_2(l+1)^2a^2 + \sum_{i=0}^{N-1}\frac{1}{2}\alpha_2 l^2a^2\right]\psi_{x,x}^2\,dx\,dy + \int\int_A \left[\sum_{i=0}^{N-1}\alpha_1(l+1)^2a^2 + \sum_{i=0}^{N-1}\frac{3}{2}\alpha_2(l+1)^2a^2 + \sum_{i=0}^{N-1}\frac{1}{2}\alpha_2 l^2a^2\right]\psi_{y,y}^2\,dx\,dy \\
& + \int\int_A N\alpha_2\psi_x^2\,dx\,dy + \int\int_A N\alpha_2\psi_y^2\,dx\,dy \\
& + \int\int_A N\alpha_2 w_{,x}^2\,dx\,dy + \int\int_A N\alpha_2 w_{,y}^2\,dx\,dy \\
& + \int\int_A Na\alpha_2\psi_{x,x}\psi_x\,dx\,dy - \int\int_A Na\alpha_2\psi_{x,x}w_{,x}\,dx\,dy \\
& - \int\int_A 2N\alpha_2\psi_x w_{,x}\,dx\,dy + \int\int_A Na\alpha_2\psi_{y,y}\psi_y\,dx\,dy \\
& - \int\int_A Na\alpha_2\psi_{y,y}w_{,y}\,dx\,dy - \int\int_A 2N\alpha_2\psi_y w_{,y}\,dx\,dy \\
& + \int\int_A \sum_{i=0}^{N-1}\alpha_2(l+1)^2a^2\psi_{x,y}^2\,dx\,dy \\
& + \int\int_A \sum_{i=0}^{N-1}(l+1)^2a^2\psi_{y,x}^2\,dx\,dy \\
& + \int\int_A \sum_{i=0}^{N-1}2\alpha_2(l+1)^2a^2\psi_{x,x}\psi_{y,y}\,dx\,dy \\
& + \int\int_A \sum_{i=0}^{N-1}2\alpha_2(l+1)^2a^2\psi_{x,y}\psi_{y,x}\,dx\,dy \\
& + \int\int_A \left(N\alpha_2 + \frac{\alpha_2}{2}\right)u_{,y}^2\,dx\,dy + \int\int_A \left(N\alpha_2 + \frac{\alpha_2}{2}\right)v_{,x}^2\,dx\,dy \\
& + \int\int_A \left(2N\alpha_2 + \alpha_2 + 2N\alpha_1 v^2 + 4N\alpha_2 v^2 - 4N\alpha_2 v\right)u_{,x}v_{,y}\,dx\,dy + \int\int_A (2N\alpha_2 + \alpha_2)u_{,y}v_{,x}\,dx\,dy \\
& + \int\int_A \left[\sum_{i=0}^{N-1}\frac{1}{2}\alpha_2(l+1)^2a^2v^2 + \sum_{i=0}^{N-1}\frac{1}{2}\alpha_2 l^2a^2v^2\right]u_{,xx}^2\,dx\,dy \\
& + \int\int_A \left[\sum_{i=0}^{N-1}\frac{1}{2}\alpha_2(l+1)^2a^2v^2 + \sum_{i=0}^{N-1}\frac{1}{2}\alpha_2 l^2a^2v^2\right]v_{,xx}^2\,dx\,dy \\
& + \int\int_A \left[\sum_{i=0}^{N-1}\alpha_2(l+1)^2a^2v^2 + \sum_{i=0}^{N-1}\alpha_2 l^2a^2v^2\right]u_{,xx}v_{,xy}\,dx\,dy \\
& + \int\int_A N\alpha_2 a(v^2 - v)u_{,x}u_{,xx}\,dx\,dy \\
& + \int\int_A N\alpha_2 a(v^2 - v)u_{,x}v_{,xy}\,dx\,dy \\
& + \int\int_A \left[\sum_{i=0}^{N-1}\frac{1}{2}\alpha_2(l+1)^2a^2v^2 + \sum_{i=0}^{N-1}\frac{1}{2}\alpha_2 l^2a^2v^2\right]v_{,yy}^2\,dx\,dy \\
& + \int\int_A \left[\sum_{i=0}^{N-1}\frac{1}{2}\alpha_2(l+1)^2a^2v^2 + \sum_{i=0}^{N-1}\frac{1}{2}\alpha_2 l^2a^2v^2\right]u_{,xy}^2\,dx\,dy \\
& + \int\int_A \left[\sum_{i=0}^{N-1}\alpha_2(l+1)^2a^2v^2 + \sum_{i=0}^{N-1}\alpha_2 l^2a^2v^2\right]u_{,xy}v_{,yy}\,dx\,dy
\end{aligned}$$

$$+\int\int_A N\alpha_2 a(\nu^2-\nu)v_{,y}v_{,yy}\,dx\,dy$$
$$+\int\int_A N\alpha_2 a(\nu^2-\nu)v_{,y}v_{,xy}\,dx\,dy$$
$$+\int\int_A N\alpha_2 a\nu^2 u_{,xx}v_{,y}\,dx\,dy+\int\int_A N\alpha_2 a\nu^2 v_{,xy}v_{,y}\,dx\,dy$$
$$+\int\int_A N\alpha_2 a\nu^2 u_{,xy}u_{,x}\,dx\,dy+\int\int_A N\alpha_2 a\nu^2 v_{,yy}u_{,x}\,dx\,dy \tag{4}$$

The work of external forces, W, is

$$W=\int\int_i w(x,y,t)q(x,y,t)\,dx\,dy+\int_S (Pu+Qw+M\psi)\,ds \tag{5}$$

where S is the geometry boundary, q the applied dynamic loading density, P the axial force, Q the shear force, and M the bending moment.

B. Equations of Motion

The equations of motions for the platelike nanostructured materials can be obtained through Hamilton's stationary principle. Hamilton's principle between two time stages t_1 and t_2 can be mathematically expressed as

$$\delta\int_1^2 (U-W-T)\,dt=0 \tag{6}$$

Substituting Eqs. (2), (4), and (5) into Eq. (6) and performing the variation, we obtain the equations of motion of the plate as follows.

For δu:

$$-2\left(N\alpha_2(1-\nu)^2+(\alpha_1+\alpha_2)\left(N\nu^2+N+\frac{1}{2}\right)\right)\frac{\partial^2 u}{\partial x^2}$$
$$-2\alpha_2\left(N+\frac{1}{2}\right)\frac{\partial^2 u}{\partial y^2}-\left(4N\alpha_2+2\alpha_2+2N\alpha_1\nu^2+4N\alpha_2\nu^2\right.$$
$$\left.-4N\alpha_2\nu\right)\frac{\partial^2 v}{\partial x\partial y}+\left(\sum_{i=0}^{N-1}\alpha_2(l+1)^2a^2\nu^2+\sum_{i=0}^{N-1}\alpha_2 l^2a^2\nu^2\right)\frac{\partial^4 u}{\partial x^4}$$
$$+\left(\sum_{i=0}^{N-1}\alpha_2(l+1)^2a^2\nu^2+\sum_{i=0}^{N-1}\alpha_2 l^2a^2\nu^2\right)\frac{\partial^4 v}{\partial x^3\partial y}$$
$$+\left(\sum_{i=0}^{N-1}\alpha_2(l+1)^2a^2\nu^2+\sum_{i=0}^{N-1}\alpha_2 l^2a^2\nu^2\right)\frac{\partial^4 u}{\partial x^2\partial y^2}$$
$$+\left(\sum_{i=0}^{N-1}\alpha_2(l+1)^2a^2\nu^2+\sum_{i=0}^{N-1}\alpha_2 l^2a^2\nu^2\right)\frac{\partial^4 v}{\partial x\partial y^3}$$
$$-N\alpha_2 a(\nu^2-\nu)\frac{\partial^3 v}{\partial x^2\partial y}+N\alpha_2 a(\nu^2-\nu)\frac{\partial^3 v}{\partial x\partial y^2}$$
$$+N\alpha_2 a\nu^2\frac{\partial^3 v}{\partial x^2\partial y}-N\alpha_2 a\nu^2\frac{\partial^3 v}{\partial x\partial y^2}+(2N+1)\rho a\ddot{u}$$
$$-\left(\sum_{i=-N}^{N} l^2\right)\rho a^3\nu^2\frac{\partial^2\ddot{u}}{\partial x^2}-\left(\sum_{i=-N}^{N} l^2\right)\rho a^3\nu^2\frac{\partial^2\ddot{v}}{\partial x\partial y}=0 \tag{7a}$$

For δv:

$$-2\left(N\alpha_2(1-\nu)^2+(\alpha_1+\alpha_2)\left(N\nu^2+N+\frac{1}{2}\right)\right)\frac{\partial^2 v}{\partial y^2}$$
$$-2\alpha_2\left(N+\frac{1}{2}\right)\frac{\partial^2 v}{\partial x^2}-\left(4N\alpha_2+2\alpha_2+2N\alpha_1\nu^2+4N\alpha_2\nu^2\right.$$
$$\left.-4N\alpha_2\nu\right)\frac{\partial^2 u}{\partial x\partial y}+\left(\sum_{i=0}^{N-1}\alpha_2(l+1)^2a^2\nu^2+\sum_{i=0}^{N-1}\alpha_2 l^2a^2\nu^2\right)$$
$$\times\frac{\partial^4 v}{\partial y^4}+\left(\sum_{i=0}^{N-1}\alpha_2(l+1)^2a^2\nu^2+\sum_{i=0}^{N-1}\alpha_2 l^2a^2\nu^2\right)\frac{\partial^4 u}{\partial x^3\partial y}$$
$$+\left(\sum_{i=0}^{N-1}\alpha_2(l+1)^2a^2\nu^2+\sum_{i=0}^{N-1}\alpha_2 l^2a^2\nu^2\right)\frac{\partial^4 v}{\partial x^2\partial y^2}$$
$$+\left(\sum_{i=0}^{N-1}\alpha_2(l+1)^2a^2\nu^2+\sum_{i=0}^{N-1}\alpha_2 l^2a^2\nu^2\right)\frac{\partial^4 u}{\partial x\partial y^3}$$
$$+N\alpha_2 a(\nu^2-\nu)\frac{\partial^3 u}{\partial x^2\partial y}+N\alpha_2 a(\nu^2-\nu)\frac{\partial^3 u}{\partial x\partial y^2}$$
$$-N\alpha_2 a\nu^2\frac{\partial^3 v}{\partial x^2\partial y}+N\alpha_2 a\nu^2\frac{\partial^3 v}{\partial x\partial y^2}+(2N+1)\rho a\ddot{v}$$
$$-\left(\sum_{i=-N}^{N} l^2\right)\rho a^3\nu^2\frac{\partial^2\ddot{v}}{\partial y^2}-\left(\sum_{i=-N}^{N} l^2\right)\rho a^3\nu^2\frac{\partial^2\ddot{u}}{\partial x\partial y}=0 \tag{7b}$$

For δw:

$$-2N\alpha_2\frac{\partial^2 w}{\partial x^2}-2N\alpha_2\frac{\partial^2 w}{\partial y^2}+Na\alpha_2\frac{\partial^2\psi_x}{\partial x^2}+2N\alpha_2\frac{\partial\psi_x}{\partial x}$$
$$+Na\alpha_2\frac{\partial^2\psi_x}{\partial y^2}+2N\alpha_2\frac{\partial\psi_y}{\partial y}+(2N+1)\rho a\ddot{w}-q=0 \tag{7c}$$

For $\delta\psi_x$:

$$-2\left(\sum_{i=0}^{N-1}\alpha_1(1+l)^2a^2+\frac{3}{2}\sum_{i=0}^{N-1}\alpha_2(1+l)^2a^2+\frac{1}{2}\sum_{i=0}^{N-1}\alpha_2 l^2a^2\right)$$
$$\times\frac{\partial^2\psi_x}{\partial x^2}+2N\alpha_2\psi_x+Na\alpha_2\frac{\partial^2 w}{\partial x^2}-2N\alpha_2\frac{\partial w}{\partial x}$$
$$-2\sum_{i=0}^{N-1}\alpha_2(1+l)^2a^2\frac{\partial^2\psi_x}{\partial y^2}-4\sum_{i=0}^{N-1}\alpha_2(1+l)^2a^2\frac{\partial^2\psi_y}{\partial x\partial y}$$
$$+\sum_{i=-N}^{N}(\rho a^3 l^2)\ddot{\psi}_x=0 \tag{7d}$$

For $\delta\psi_y$:

$$-2\left(\sum_{i=0}^{N-1}\alpha_1(1+l)^2a^2+\frac{3}{2}\sum_{i=0}^{N-1}\alpha_2(1+l)^2a^2+\frac{1}{2}\sum_{i=0}^{N-1}\alpha_2 l^2a^2\right)$$
$$\times\frac{\partial^2\psi_y}{\partial x^2}+2N\alpha_2\psi_y+Na\alpha_2\frac{\partial^2 w}{\partial y^2}-2N\alpha_2\frac{\partial w}{\partial y}$$
$$-2\sum_{i=0}^{N-1}\alpha_2(1+l)^2a^2\frac{\partial^2\psi_y}{\partial x^2}-4\sum_{i=0}^{N-1}\alpha_2(1+l)^2a^2\frac{\partial^2\psi_x}{\partial x\partial y}$$
$$+\sum_{i=-N}^{N}(\rho a^3 l^2)\ddot{\psi}y_x=0 \tag{7e}$$

III. Comparison of the Nanoplate Model with the Corresponding Lattice Model

To evaluate the accuracy of the nanoplate model, the displacement equations of motion, Eqs. (7a–7e), are used to study the propagation

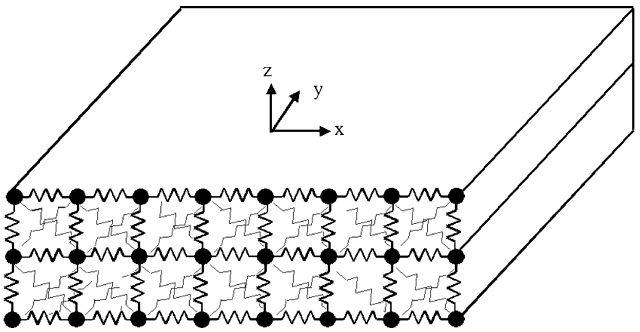

Fig. 3 Three-layered nanostructured material for dispersion analysis.

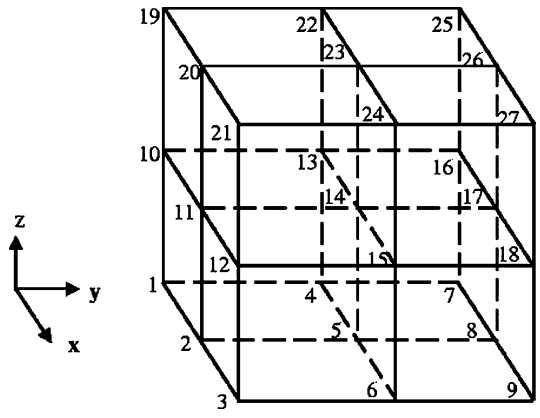

Fig. 4 Representative cell of lattice model.

of plane harmonic waves in the nanoplate and the resulting phase velocities are compared with those according to the lattice model. We consider harmonic waves propagating in the x direction in a three-layered nanomaterial as shown in Fig. 3. In this example, the plane strain condition parallel to the x–y plane is adopted. We first derive the dispersion relations with the lattice model and then with the nanoplate model.

A. Lattice model

Harmonic wave propagation in the lattice model can be analyzed using a representative cell as shown in Fig. 4. This representative cell can be arbitrarily chosen in the x and y directions because the plane strain condition is assumed in the y direction and the dimension in the x direction is infinite. The equations of motion at middle cell points 14, 5, and 23 along the thickness direction can be formulated with Newton's second law as

$$m\frac{\mathrm{d}^2u(14)}{\mathrm{d}t^2} = -\alpha_1[2u(14) - u(13) - u(15)] + \frac{\alpha_2}{2}[u(12) - u(14) - v(12) + v(14)] + \frac{\alpha_2}{2}[u(18) - u(14) + v(18) - v(14)] + \frac{\alpha_2}{2}[u(16) - u(14) - v(16) + v(14)] + \frac{\alpha_2}{2}[u(10) - u(14) + v(10) - v(14)] + \frac{\alpha_2}{2}[u(22) - u(14) - w(12) + w(14)] + \frac{\alpha_2}{2}[u(4) - u(14) + w(4) - w(14)] + \frac{\alpha_2}{2}[u(6) - u(14) - w(6) + w(14)] + \frac{\alpha_2}{2}[u(24) - u(14) + w(24) - w(14)] \tag{8a}$$

$$m\frac{\mathrm{d}^2v(14)}{\mathrm{d}t^2} = -\alpha_1[2v(14) - v(17) - v(11)] + \frac{\alpha_2}{2}[-u(12) + u(14) + v(12) - v(14)] + \frac{\alpha_2}{2}[u(18) - u(14) + v(18) - v(14)] + \frac{\alpha_2}{2}[-u(16) + u(14) + v(16) - v(14)] + \frac{\alpha_2}{2}[u(10) - u(14) + v(10) - v(14)] + \frac{\alpha_2}{2}[v(20) - v(14) - w(20) + w(14)] + \frac{\alpha_2}{2}[v(2) - v(14) + w(2) - w(14)] + \frac{\alpha_2}{2}[v(8) - v(14) - w(8) + w(14)] + \frac{\alpha_2}{2}[v(26) - v(14) + w(26) - w(14)] \tag{8b}$$

$$m\frac{\mathrm{d}^2w(14)}{\mathrm{d}t^2} = -\alpha_1[2w(14) - w(23) - w(5)] + \frac{\alpha_2}{2}[-v(20) + v(14) + w(20) - w(14)] + \frac{\alpha_2}{2}[v(2) - v(14) + w(2) - w(14)] + \frac{\alpha_2}{2}[-v(8) + v(14) + w(8) - w(14)] + \frac{\alpha_2}{2}[v(26) - v(14) + w(26) - w(14)] + \frac{\alpha_2}{2}[-u(22) + u(14) + w(12) - w(14)] + \frac{\alpha_2}{2}[u(4) - u(14) + w(4) - w(14)] + \frac{\alpha_2}{2}[-u(6) + u(14) + w(6) - w(14)] + \frac{\alpha_2}{2}[u(24) - u(14) + w(24) - w(14)] \tag{8c}$$

$$m\frac{\mathrm{d}^2u(5)}{\mathrm{d}t^2} = -\alpha_1[2u(5) - u(4) - u(6)] + \frac{\alpha_2}{2}[u(3) - u(5) - v(3) + v(5)] + \frac{\alpha_2}{2}[u(9) - u(5) + v(9) - v(5)] + \frac{\alpha_2}{2}[u(7) - u(5) - v(7) + v(5)] + \frac{\alpha_2}{2}[u(1) - u(5) + v(1) - v(5)] + \frac{\alpha_2}{2}[u(13) - u(5) - w(13) + w(5)] + \frac{\alpha_2}{2}[u(15) - u(9) + w(15) - w(5)] \tag{8d}$$

$$m\frac{\mathrm{d}^2v(5)}{\mathrm{d}t^2} = -\alpha_1[2v(5) - v(2) - v(8)] + \frac{\alpha_2}{2}[-u(3) + u(5) + v(3) - v(5)] + \frac{\alpha_2}{2}[u(9) - u(5) + v(9) - v(5)] + \frac{\alpha_2}{2}[-u(7) + u(5) + v(7) - v(5)] + \frac{\alpha_2}{2}[u(1) - u(5) + v(1) - v(10)] + \frac{\alpha_2}{2}[v(11) - v(5) - w(11) + w(5)] + \frac{\alpha_2}{2}[v(17) - v(5) + w(17) - w(5)] \tag{8e}$$

$$m\frac{\mathrm{d}^2w(5)}{\mathrm{d}t^2} = -\alpha_1[w(5) - w(14)] + \frac{\alpha_2}{2}[-v(11) + v(5) + w(11) - w(5)] + \frac{\alpha_2}{2}[v(17) - v(5) + w(17) - w(5)] + \frac{\alpha_2}{2}[-u(13) + u(5) + w(13) - w(5)] + \frac{\alpha_2}{2}[u(15) - u(5) + w(15) - w(5)] \tag{8f}$$

$$m\frac{\mathrm{d}^2u(23)}{\mathrm{d}t^2} = -\alpha_1[2u(23) - u(24) - u(22)] + \frac{\alpha_2}{2}[u(21) - u(23) - v(21) + v(23)] + \frac{\alpha_2}{2}[u(27) - u(23) + v(27) - v(23)] + \frac{\alpha_2}{2}[u(25) - u(23) - v(25) + v(23)] + \frac{\alpha_2}{2}[u(19) - u(23)$$

$$+ v(19) - v(23)] + \frac{\alpha_2}{2}[u(13) - u(23) + w(13) - w(23)]$$
$$+ \frac{\alpha_2}{2}[u(15) - u(23) + w(15) + w(23)] \quad (8g)$$

$$m\frac{d^2v(23)}{dt^2} = -\alpha_1[2v(23) - v(20) - v(26)] + \frac{\alpha_2}{2}[-u(21) + u(23)$$
$$+ v(21) - v(23)] + \frac{\alpha_2}{2}[u(27) - u(23) + v(27) - v(23)]$$
$$+ \frac{\alpha_2}{2}[-u(25) + u(23) + v(25) - v(23)] + \frac{\alpha_2}{2}[u(19) - u(23)$$
$$+ v(19) - v(23)] + \frac{\alpha_2}{2}[v(11) - v(23) + w(11) - w(23)]$$
$$+ \frac{\alpha_2}{2}[v(17) - v(23) - w(17) + w(23)] \quad (8h)$$

$$m\frac{d^2w(23)}{dt^2} = -\alpha_1[w(23) - w(14)] + \frac{\alpha_2}{2}[v(11) - v(23) + w(11)$$
$$- w(23)] + \frac{\alpha_2}{2}[-v(17) + v(23) + w(17) - w(23)]$$
$$+ \frac{\alpha_2}{2}[u(13) - u(23) + w(13) - w(23)]$$
$$+ \frac{\alpha_2}{2}[-u(15) + u(23) + w(15) - w(23)] \quad (8i)$$

Also, angular frequency ω is related to phase velocity c by the relation

$$kc = \omega \quad (12)$$

Motivated by the wave propagation solution form for a two-layered continuum medium,[16] the wave propagation solution of the lattice model can be assumed of the following form:

$$u_1(n, p, 0) = A_1 \exp[i(kna - \omega t)] \quad (13a)$$
$$w_1(n, p, 0) = B_1 \exp[i(kna - \omega t)] \quad (13b)$$
$$u_2(n, p, 1) = A_2 \exp[i(kna - \omega t)] \quad (13c)$$
$$w_2(n, p, 1) = B_2 \exp[i(kna - \omega t)] \quad (13d)$$
$$u_3(n, p, -1) = A_3 \exp[i(kna - \omega t)] \quad (13e)$$
$$w_3(n, p, -1) = B_3 \exp[i(kna - \omega t)] \quad (13f)$$

In Eqs. (13a–13f), u_1, w_1, u_2, w_2, u_3, and w_3 are the displacement expressions for middle, upper, and lower lattice layers, respectively. The substitution of Eqs. (13a–13f) in the displacement equations of motion (8) yields a system of six homogeneous equations for A_1, A_2, A_3, B_1, B_2, and B_3. The dispersion equation is obtained by requiring that the determinant of coefficients vanishes. The resulting dispersion equation can be written as

$$\begin{vmatrix}
m\omega^2 - 2\alpha_1 + 2\alpha_1\cos ka - 4\alpha_2 + 2\alpha_2\cos ka & 0 & \alpha_2\cos ka & i\alpha_2\sin ka & \alpha_2\cos ka & -i\alpha_2\sin ka \\
0 & m\omega^2 - 2\alpha_i - 4\alpha_2 & i\alpha_2\sin ka & \alpha_1 + \alpha_2 + \alpha_2\cos ka & -i\alpha_2\sin ka & \alpha_1 + \alpha_2 + \alpha_2\cos ka \\
\alpha_2\cos ka & -i\alpha_1\sin ka & m\omega^2 - 2\alpha_1 + 2\alpha_1\cos ka - 3\alpha_2 + 2\alpha_2\cos ka & 0 & 0 & 0 \\
-i\alpha_2\sin ka & \alpha_1 + \alpha_2 + \alpha_2\cos ka & 0 & m\omega^2 - \alpha_1 - 2\alpha_2 & 0 & 0 \\
\alpha_2\cos ka & i\alpha_2\sin ka & 0 & 0 & m\omega^2 - 2\alpha_1 + 2\alpha_1\cos ka - 3\alpha_2 + 2\alpha_2\cos ka & 0 \\
i\alpha_2\sin k & \alpha_1 + \alpha_2 + \alpha_2\cos ka & 0 & 0 & 0 & m\omega^2 - \alpha_1 - 2\alpha_2
\end{vmatrix} = 0 \quad (14)$$

where $u(14)$, $v(14)$, and $w(14)$ are the x, y, and z displacements, respectively, at discrete point 14, etc.

We also introduce (m, n, l) in the following way to identify the point positions near point 14:

$$x = ma, \qquad y = na, \qquad z = la \quad (9)$$

where n, p, and $l = -1$, 0, or 1. For example, we can use (1, 0, 0) to identify the position of point 15, etc.

For a plane harmonic wave propagating in the x direction, displacements u and w can be assumed to be in the following form:

$$A\exp[i(kma - \omega t)] \quad (10)$$

with displacement $v = 0$. In Eq. (10), ω is angular frequency, A is wave amplitude, and k is wave number. Wave number k is related to wave length λ as

$$k\lambda = 2\pi \quad (11)$$

Equation (14) it can be solved numerically for angular frequencies for each given wave number.

B. Nanoplate model

For the nanoplate model, we assume the harmonic wave solutions of the form[17]

$$u = A\exp[i(kx - \omega t)] \quad (15a)$$
$$w = B\exp[i(kx - \omega t)] \quad (15b)$$
$$\psi_x = C\exp[i(kx - \omega t)] \quad (15c)$$

with $v = 0$ and $\psi_y = 0$. Substitution of these expressions in the equations of motion (7a–7e) yields

$$A\left\{\begin{array}{l} 2\left[N\alpha_2(1-\nu)^2 + (\alpha_1+\alpha_2)\left(N\nu^2 + N + \frac{1}{2}\right)\right]k^2 \\ \quad + \left[\sum_{i=0}^{N-1}\alpha_2(l+1)^2a^2\nu^2 + \sum_{i=0}^{N-1}\alpha_2 l^2a^2\nu^2\right] \\ \quad \times k^4 - 3\rho a\omega^2 - 2\rho a^3\nu^2k^2\omega^2 \end{array}\right\} = 0 \quad (16a)$$

$$B\left[2\alpha_2 k^2 a - 3\rho a^2\omega^2\right] + C\left[i2\alpha_2 ka - a_2 k^2 a^2\right] = 0 \tag{16b}$$

$$B\left[-i2\alpha_2 ka - \alpha_2 k^2 a^2\right] + C\left[2\alpha_2 a + 2(\alpha_1 + 3\alpha_2/2)k^2 a^3 - 2\rho a^4\omega^2\right] = 0 \tag{16c}$$

From Eq. (16a), we can obtain the dispersion equation for the longitudinal wave as

$$\beta = \sqrt{\frac{2\left(N\alpha_2(1-\nu)^2 + (\alpha_1+\alpha_2)\left(N\nu^2 + N + \frac{1}{2}\right)\right) + \left(\sum_{i=0}^{N-1}\alpha_2(l+1)^2\nu^2 + \sum_{i=0}^{N-1}\alpha_2 l^2\nu^2\right)\xi^2}{3\alpha_2 + 2\nu^2\xi^2\alpha_2}} \tag{17}$$

where

$$\beta = c/(\alpha_2/a\rho)^{\frac{1}{2}} \tag{18}$$

is dimensionless wave velocity and $\xi = ka$ is dimensionless wave number.

The dispersion equation for the flexural wave is obtained from Eqs. (16b) and (16c) with the result

$$\begin{vmatrix} 2\alpha_2 k^2 a - 3\rho a^2\omega^2 & i2\alpha_2 ka - \alpha_2 k^2 a^2 \\ -i2\alpha_2 ka - \alpha_2 k^2 a^2 & 2\alpha_2 a + 2(\alpha_1 + 3\alpha_2/2)k^2 a^3 - 2\rho a^4\omega^2 \end{vmatrix} = 0 \tag{19}$$

which is solved numerically for the angular frequency.

C. Comparison of Results

The dispersion curves obtained with the lattice model and the nanoplate model, respectively, are plotted in Fig. 5 in which the parameters used are $\alpha_1 = 2.02$ N/m, $\alpha_2 = 1.10$ N/m (Ref. 13), and $\nu = 0.26$. For the first mode, the flexural wave, good agreement in phase velocities according to these two models is noted up to $ka \approx 1.5$, which corresponds to a wavelength of about $4a$. For the longitudinal wave, the nanoplate solution agrees with the lattice model solution for wavelengths greater than $16a$.

IV. Cylindrical Bending of a Nanoplate

To assess the ability of the nanoplate model in predicting the deformation of platelike nanomaterials and evaluate the applicability of classical continuum theory (continuum theory without considering the nanosize effect) in the prediction of Young's modulus from nanoscale experiments, cylindrical bending of a three-layered cantilever nanoplate subjected to a uniform transverse load q, as shown in Fig. 6, is investigated. Three models are considered, namely, the Mindlin plate theory, the nanoplate model, and the lattice model. The plate is composed of three atom layers, and the length of the plate is chosen as $L = 200a$, which will allow the continuum treatment along the x direction. In this analysis, $a = 1.74 \times 10^{-10}$ m. The length along the y direction is assumed to be infinite.

A. Mindlin Plate Theory

In the continuum Mindlin[15] plate theory, the governing equations are[18]

$$A_{55}\left(\frac{\partial\psi_x}{\partial x} + \frac{\partial^2 w}{\partial x^2}\right) + q = 0 \tag{20a}$$

$$D_{11}\frac{\partial^2\psi_x}{\partial x^2} - A_{55}\left(\psi_x + \frac{\partial w}{\partial x}\right) = 0 \tag{20b}$$

where

$$D_{11} = Eh^3/12(1-\nu^2), \qquad A_{55} = hE/2(1+\nu) \tag{21}$$

where E is Young's modulus, v is Poisson's ratio, and h is the thickness of the plate. Following Ref. 10, the thickness of the continuum that represents a single atom layer is defined to be equal to the atomic spacing a. Thus, for the three-layered cantilever nanoplate, the thickness is $h = 3a$.

The boundary conditions are, at $x = 0$,

$$w = 0, \qquad \psi_x = 0 \tag{22a}$$

and at $x = L$,

$$M_x = 0, \qquad Q_x = 0 \tag{22b}$$

where M_x and Q_x are resultant moment and shear force, respectively. They are related to the displacement w and ψ_x through

$$M_x = -D_{11}\frac{\mathrm{d}\psi_x}{\mathrm{d}x} \tag{23a}$$

$$Q_x = A_{55}\gamma_{xz} = A_{55}\left(\frac{\mathrm{d}w}{\mathrm{d}x} + \psi_x\right) \tag{23b}$$

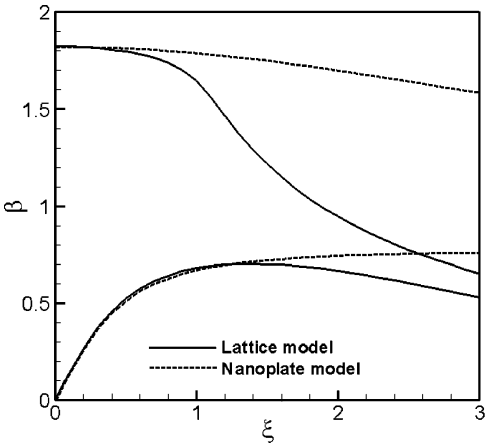

Fig. 5 Propagation of plane harmonic wave in a three-layered nanomaterial (modes 1 and 2).

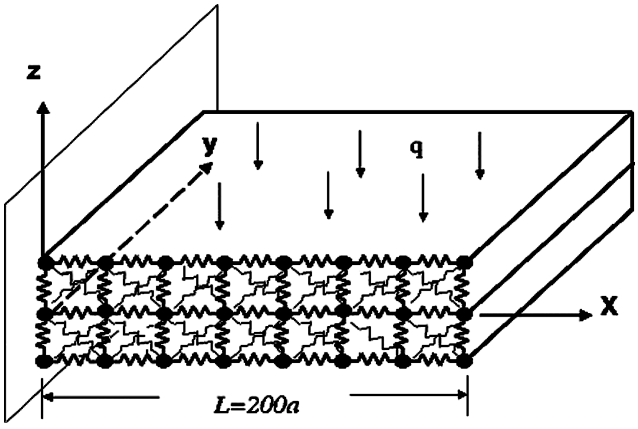

Fig. 6 Cylindrical bending of three-layered nanomaterial subjected to a uniform transverse load q.

Solving Eqs. (20a) and (20b) with boundary conditions (22a) and (22b), we obtain the deflection of the plate as

$$w = (1/24)(q/D_{11})x^4 - (1/6)(q/D_{11})Lx^3 + \left[-q/2A_{55} + (1/4)(q/D_{11})L^2\right]x^2 + (q/A_{55})Lx \quad (24)$$

The maximum deflection occurs at $x = L$:

$$w_{\max} \tfrac{1}{8}(q/D_{11})L^4 + \left(qL^2/2A_{55}\right) \quad (25)$$

B. Nanoplate Model

For cylindrical bending, nanoplate field equations given by Eqs. (7a–7e) reduce to

$$-2N\alpha_2\frac{\mathrm{d}^2w}{\mathrm{d}x^2} + Na\alpha_2\frac{\mathrm{d}^2\psi_x}{\mathrm{d}x^2} + 2N\alpha_2\frac{\mathrm{d}\psi_x}{\mathrm{d}x} - q = 0 \quad (26a)$$

$$A\frac{\mathrm{d}^2\psi_x}{\mathrm{d}x^2} + 2N\alpha_2\left(\psi_x - \frac{\mathrm{d}w}{\mathrm{d}x}\right) + Na\alpha_2\frac{\mathrm{d}^2w}{\mathrm{d}x^2} = 0 \quad (26b)$$

where

$$A = -2\left[\sum_{i=0}^{N-1}\alpha_1(1+l)^2a^2 + \frac{3}{2}\sum_{i=0}^{N-1}\alpha_2(1+l)^2a^2 + \frac{1}{2}\sum_{i=0}^{N-1}\alpha_2l^2a^2\right] \quad (27)$$

The boundary conditions are the same as conditions (22a) and (22b). The relation between M_x and Q_x and the displacements w and ψ_x are obtained from the taking the variation of Eq. (6). We have

$$Q_x = 2N\alpha_2\frac{\mathrm{d}w}{\mathrm{d}x} - Na\alpha_2\frac{\mathrm{d}\psi_x}{\mathrm{d}x} - 2N\alpha_2\psi_x \quad (28a)$$

$$M_x = -A\frac{\mathrm{d}\psi_x}{\mathrm{d}x} + Na\alpha_2\psi_x - Na\alpha_2\frac{\mathrm{d}w}{\mathrm{d}x} \quad (28b)$$

Solving Eqs. (26a) and (26b) with boundary conditions (28a) and (28b), we obtain the deflection of the plate as

$$w = \frac{Na^2\alpha_2 + 2A}{4N\alpha_2}\left(-\frac{q}{Na^2\alpha_2 + 2A}x^2 + C_1x\right) + \frac{a}{2}\left(-\frac{1}{3}\frac{q}{Na^2\alpha_2 + 2A}x^3 + \frac{1}{2}C_1x^2 + C_2x\right) - \frac{1}{12}\frac{q}{Na^2\alpha_2 + 2A}x^4 + \frac{1}{6}C_1x^3 + \frac{1}{2}C_2x^2 - \frac{qa}{4N\alpha_2}x \quad (29)$$

where

$$C_1 = \frac{2qL + qa}{Na^2\alpha_2 + 2A}$$

$$C_2 = \left[\left(-LA - \frac{Na^3 + 2Aa}{4} - \frac{Na^2\alpha_2L}{2}\right)\frac{2qL + qA}{Na^2\alpha_2 + 2A} + \frac{2qL^2 + 2qaL + qa^2}{4}\right]\Big/\left(A + \frac{Na^2\alpha_2}{2}\right)$$

The maximum deflection occurs at $x = L$:

$$w_{\max} = \frac{Na^2\alpha_2 + 2A}{4N\alpha_2}\left(-\frac{q}{Na^2\alpha_2 + 2A}L^2 + C_1L\right) + \frac{a}{2}\left(-\frac{1}{3}\frac{q}{Na^2\alpha_2 + 2A}L^3 + \frac{1}{2}C_1L^2 + C_2L\right) - \frac{1}{12}\frac{q}{Na^2\alpha_2 + 2A}L^4 + \frac{1}{6}C_1L^3 + \frac{1}{2}C_2L^2 - \frac{qa}{4N\alpha_2}L$$

C. Lattice Model

The analysis with the lattice model is performed with the aid of the commercial finite element code ANSYS. Element COMBIN 14 is used to model the first and second neighbor reaction force springs between atoms. In view of the nature of cylindrical bending, a representative strip of the plate, as shown in Fig. 7, is taken for analysis. Because of the repetitive requirement on representative strips, the spring constants for the elements in the front and back surfaces of the strip are half of the actual values. The displacements of the nodes in the front and back surfaces are suppressed in the y direction. The load with a magnitude of $qa^2/4$ is applied to each node in the top and bottom surfaces.

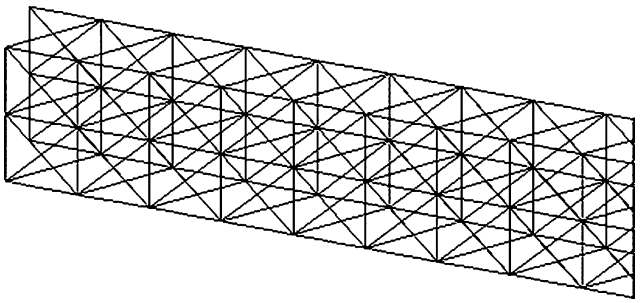

Fig. 7 Lattice model of three-layered nanomaterial subjected to a uniform transverse load q.

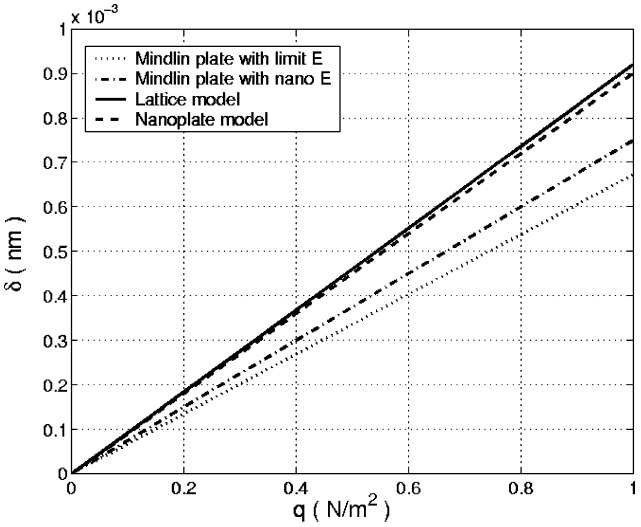

Fig. 8 Maximum deflection d, which appears at the right end of the plate, of three-layered nanomaterial as a function of uniform transverse load q.

Figure 8 shows the maximum deflection δ of the three-layered nanoplate as a function of a uniform transverse load q. For the lattice model, δ is chosen as the deflection of the middle node at the right end of the plate. In applying the Mindlin plate theory, both Young's modulus E according to the lattice model (see Ref. 10) and its continuum limit E_c are used. It is evident that, at a fixed transverse load q, the predicted maximum deflection obtained with the nanoplate model is very close to that obtained with the lattice model, having a maximum difference of 3%. In contrast, the Mindlin plate theory underestimates the maximum deflection by 26% when E_c is used and by 18.5% when E is used. This implies that if an experimentally measured deflection is used to determine the Young's modulus of a nanoplate with the aid of the Mindlin plate theory, the Young's modulus will be underestimated.

V. Conclusions

A nanoplate model that can be used to analyze the deformation of platelike nanomaterials has been developed based on a semicontinuum approach. This model retains the discrete properties of the material along the thickness dimension while treating it as a continuum along the in-plane dimensions. From the analysis of dispersion of harmonic waves, it was found that the present model

yields very good agreement with the lattice model for wavelengths greater than 4*a* and 16*a* for the flexural wave and the longitudinal wave, respectively.

From the study in cylindrical bending of a three-layered cantilever nanoplate, it was found that the nanoplate model can predict the deflection with reasonable accuracy as compared with the lattice model. It was also noted that the continuum Mindlin plate theory tends to overestimate the bending stiffness of the nanoplate. Consequently, when used in data analyses, the continuum Mindlin plate theory will underestimate the Young's modulus of the nanoplate.

Acknowledgment

This work was supported by NASA Langley Research Center Grant NAG-1-01073 to Purdue University.

References

[1]Vettiger, P., Brugger, J., Despont, M., Drechsler, U., Drig, U., Häberle, W., Lutwyche, M., Rothuizen, H., Stutz, R., Widmer, R., and Binnig, G., "Ultrahigh Density, High-Data-Rate NEMS-based AFM Data Storage System," *Microelectronic Engineering*, Vol. 46, Nos. 1–4, 1999, pp. 11–17.

[2]Dai, H., Hafner, J. H., Rinzler, A. G., Colbert, D. T., and Smalley, R. E., "Nanotubes as Nanoprobes in Scanning Probe Microscopy," *Nature*, Vol. 384, No. 6605, 1996, pp. 147–151.

[3]Stevens, R., Frederick, N., Smith, B., Morse, D., Stucky, G., and Hansma, P., "Carbon Nanotubes as Probes for Atomic Force Microscopy," *Nanotechnology*, Vol. 11, No. 1, 2000, pp. 1–5.

[4]Avouris, P., Hertel, T., Martel, R., Schmidt, T., Shea, H. R., and Walkup, R. E., "Carbon Nanotubes: Nanomechanics, Manipulation, and Electronic Devices," *Applied Surface Science*, Vol. 141, Nos. 3–4, 1999, pp. 201–209.

[5]Broughton, J. Q., Meli, C. A., Vashishta, P., and Kalia, R. K., "Direct Atomistic Simulation of Quartz Crystal Oscillators: Bulk Properties and Nanoscale Devices," *Physical Review B*, Vol. 56, No. 2, 1997, pp. 611–618.

[6]Rudd, R. E., and Broughton, J. Q., "Atomistic Simulation of MEMS Resonators through the Coupling of Length Scales," *Journal of Modeling and Simulation of Microsystems*, Vol. 1, No. 1, 1999, pp. 29–38.

[7]Govindjee, S., and Sackman, J. L., "On the Use of Continuum Mechanics to Estimate the Properties of Nanotubes," *Solid State Communications*, Vol. 110, No. 4, 1999, pp. 227–230.

[8]Rudd, R. E., and Broughton, J. Q., "Coupling of Length Scales and Atomistic Simulation of MEMS Devices," *Technical Proceedings of the 1998 International Conference on Modeling and Simulation of Microsystems*, Computational Publications, Cambridge, MA, 1998, pp. 287–291.

[9]Zhang, H., and Sun, C. T., "Semi-Continuum Model for Plate-Like Nanomaterials," AIAA Paper 2002-1316, April 2002.

[10]Sun, C. T., and Zhang, H., "Size-depended Elastic Moduli of Plate-Like Nanomaterials," *Journal of Applied Physics*, Vol. 93, No. 2, 2003, pp. 1212–1218.

[11]Petersen, K., and Guarnieri, C., "Young's Modulus Measurements of Thin Films Using Micromechanics," *Journal of Applied Physics*, Vol. 50, No. 11, 1979, pp. 6761–6766.

[12]Ghatak, A. K., and Kothari, L. S., *Introduction to Lattice Dynamics*, Addison–Wesley, Reading MA, 1972, pp. 1–99.

[13]Askar, A., *Lattice Dynamics Foundations of Continuum Theories*, World Scientific, Singapore, 1984, pp. 3–91.

[14]Zhang, H., "Mechanical Behavior of Nanomaterials: Modeling and Simulation," Ph.D. Dissertation, School of Aeronautics and Astronautics, Purdue Univ., West Lafayette, IN, Jan. 2004.

[15]Mindlin, R. D., "Influence of Rotatory Inertia and Shear on Flexural Motions of Isotropic, Elastic Plates," *Journal of Applied Mechanics*, Vol. 18, No. 1, 1951, pp. 31–38.

[16]Jones, J. P., "Wave Propagation in a Two-Layered Medium," *Journal of Applied Mechanics*, Vol. 31, No. 2, 1964, pp. 213–222.

[17]Sun, C. T., Achenbach, J. D., and Herrmann, D., "Continuum Theory for a Laminated Medium," *Journal of Applied Mechanics*, Vol. 35, No. 4, 1968, pp. 467–475.

[18]Whitney, J. M., and Pagano, N. J., "Shear Deformation in Heterogeneous Anistropic Plates," *Journal of Applied Mechanics*, Vol. 37, No. 4, 1970, pp. 1031–1036.

B. Sankar
Associate Editor